BUTTERWORTH HEINEMANN

Polymer Vol. 36 No. 5, pp. 987–1002, 1995

0032-3861/95/$10.00 + 0.00

High temperature polymer nanofoams based on amorphous, high T_g polyimides

Y. Charlier, J. L. Hedrick*, T. P. Russell, A. Jonas and W. Volksen
IBM Research Division, Almaden Research Center, 650 Harry Road, San Jose, CA 95120-6099, USA
(Received 13 March 1994; revised 14 July 1994)

A means of generating high temperature polymer foams which leads to pore sizes in the nanometre regime has been developed. Foams were prepared by casting block copolymers comprising a thermally stable block and a thermally labile material, such that the morphology consists of a matrix of the thermally stable material with the thermally labile material as the dispersed phase. Upon thermal treatment, the thermally unstable block undergoes thermolysis leaving pores of which the size and shape are dictated by the initial copolymer morphology. Triblock and graft copolymers comprising high glass transition temperature amorphous polyimide matrices with poly(propylene oxide), as the thermally decomposable coblock, were prepared. The copolymer synthesis was carried out through either the poly(amic alkyl ester) or poly(amic acid) precursor and subsequent cyclodehydration to the polyimide by either thermal or chemical means, respectively. Microphase-separated morphologies were observed for all copolymers, irrespective of the block lengths surveyed, by dynamic mechanical analysis. Upon decomposition of the thermally labile coblock, a 5–15% reduction in density was observed, consistent with the generation of a foam.

(Keywords: nanofoams; amorphous polyimide; morphology)

INTRODUCTION

Polyimides are currently the materials of choice for interlayer dielectrics in microelectronic applications, since polyimides, as a class of materials, best satisfy the requisite properties to survive the thermal, chemical and mechanical stresses associated with microelectronic fabrication techniques. Although polyimides meet most of the material requirements for this application, polymeric materials have many drawbacks when compared to inorganic alternatives[1]. The key advantages realized by the use of polymeric materials are improved or simplified processing conditions (i.e. spin coating) and lower dielectric constants. A reduction in the dielectric constant of the medium reduces pulse propagation delay, allowing for faster machine time as well as minimizing 'cross talk' or noise between signal lines. The improvement in 'cross talk' facilitates the design of denser structures. The semi-rigid and rigid polyimides (e.g. poly(4,4'-oxydiphenylene pyromellitimide) (PMDA/ODA) and poly[*N*,*N*'-(*p*-phenylene)biphenyltetracarboximide] (BPDA/PDA), respectively) have proven to be the most suitable materials for these applications due to their processability from the soluble poly(amic acid) precursor form and their excellent final properties after thermal cure. These properties, including low thermal expansion coefficient and high modulus, can be attributed, in part, to the liquid crystalline type of ordering in the solid state manifested by these polyimides[2,3]. Although polyimides meet many of the material requirements, future advances in high performance computing will require improved dielectric insulators with substantially lower dielectric constants.

While there are many routes to lower the dielectric constant of polyimides, the most common approach has been by the incorporation of perfluoroalkyl groups. Examples include hexafluoroisopropylidine linkages[4], main chain perfluoroalkylene groups[5], and pendent trifluoromethyl groups[6,7]. Such modifications afford materials with dielectric constants below 3.0 and low water absorption ($\simeq$0.5%). Unfortunately, the final properties of the materials are sacrificed. The addition of pendent trifluoromethyl groups appears to have the least negative effect. However, the percentage of fluorine which can be synthetically incorporated into the polymer is limited. Other means of reducing the dielectric constant of polyimides have been demonstrated by St. Clair and co-workers[8] by chemical modification of the polymer backbone to reduce chain–chain interactions. Appropriately designed systems yielded dielectric constants in the range 2.4–2.8.

An alternative approach to lower the dielectric constant substantially, while maintaining the desired thermal and mechanical properties, is to generate a polyimide foam. The reduction in the dielectric constant results from replacing the polymer, having a dielectric constant of $\sim$3.0, with air which has a dielectric constant of 1. However, the criteria for the size of the pores or voids is stringent. It is critical that the size of the voids be much smaller than the film thickness and/or underlying

* To whom correspondence should be addressed

microelectronic features for the gain in the dielectric constant to be realized. Secondly, it is necessary for the pores to be closed cell, so as to minimize pore-interconnectivity. An open-celled structure would not necessarily have a detrimental effect on the dielectric performance of the film, but water and solvent uptake during subsequent processing would be exacerbated by the connectivity of the pores. Also, the size, interconnectivity and volume fraction of the pores can alter the mechanical properties and structural stability of the foamed material. If any of these is too large, then the foam can collapse, which essentially regenerates the original material.

Polyimide foams, which show high compressive strength, low dielectric constant, low density and good thermal stability[9], have been developed primarily for the aerospace and transportation industries. The routes to the preparation of polyimide foams include foaming agents[10–12], partial degradation generating a foaming agent[10–19], the inclusion of glass or carbon microspheres[20–24] and microwave processing[25]. Most of the high temperature polymer foams reported to date do not satisfy the requirements for applications in microelectronics due to the large void size and open nature of the cellular structure.

We have developed an alternative means of generating a high temperature polymer foam which leads to pore sizes in the nanometre regime. Foams can be prepared from block copolymers comprising a thermally stable and thermally labile material, where the latter constitutes the dispersed phase[26]. Upon thermal treatment, the thermally unstable block undergoes thermolysis, leaving pores where the size and shape of the pores are dictated by the initial copolymer morphology. Triblock copolymers comprising a poly(phenylquinoxaline) (PPQ) with either poly(propylene oxide) or poly(methyl methacrylate) as the thermally labile coblock, have been shown to produce nanofoams with dielectric constants substantially lower than the pure matrix polymer. Upon decomposition of the thermally unstable blocks, an 8–12% reduction in density was observed along with a reduction in the dielectric constant from 2.8 to 2.4 for the unfoamed and foamed PPQ, respectively. Small-angle X-ray scattering and transmission electron microscopy showed pore sizes of approximately 100 Å. Conversely, block copolymers derived from rigid and semi-rigid polyimides with either poly(methyl methacrylate) or poly(propylene oxide) did not show the expected nanofoam formation upon thermolysis of the labile coblock[27]. The rapid collapse of the foam well below the nominal glass transition temperature, T_g, was attributed to the anisotropic mechanical properties, characteristic of thin films of these ordered polyimides. The systematic introduction of flexible monomers into these otherwise rigid materials, yielded stable foams only for those samples which were amorphous and isotropic. In an effort to expand both the processing window and operating temperature of such nanofoams, high T_g amorphous polyimides have been prepared. In this article, the synthesis and characterization of block copolymers derived from either pyromellitic anhydride with 9,9′-bis(4-aminophenyl)fluorene (PMDA/FDA) or oxydiphthalic anhydride with 9,9′-bis(4-aminophenyl)fluorene (ODPA/FDA) polyimide having poly(propylene oxide) as the thermally labile coblock will be presented.

EXPERIMENTAL

Materials

N-Methyl-2-pyrrolidone (NMP), pyridine and acetic anhydride were purchased from Aldrich and used without further purification. The *N*-cyclohexyl-2-pyrrolidone (CHP) was obtained from Aldrich and vacuum distilled from P_2O_5. Oxydiphthalic anhydride (ODPA), 9,9′-bis(4-aminophenyl)fluorene (FDA) and pyromellitic dianhydride (PMDA) (Chriskev Co.) were sublimed three times prior to use. Monofunctional hydroxyl propylene oxide oligomers of nominal molecular weights 5000 and 10 000 g mol^{-1} were kindly supplied by Dow Chemical Co.

Diethyl pyromellitate diacyl chloride. PMDA (50.0 g, 0.230 mol) was suspended in 250 ml of dry ethanol and refluxed for 3 h, yielding a clear solution[28]. Evaporation of the ethanol followed by vacuum drying at 50°C for 24 h gave diethyl dihydrogen pyromellitate (mixed isomers) in quantitative yield. The material was then suspended in ~200 ml of dry ethyl acetate in a 500 ml three-necked flask equipped with magnetic stirrers, reflux condenser and N_2 bubbler. Next, oxalyl chloride (75 g, 0.591 mol) was added in three portions over a period of 8–10 h, each addition being followed by one to two drops of dimethylformamide (DMF). The DMF allowed the reaction to proceed at ambient temperature as evidenced by vigorous gas evolution. Stirring was continued overnight and the reaction was then heated to ~60°C in a water bath for an additional 6 h (total run time was ~28 h). The ethyl acetate was then stripped and the residue dried under vacuum at room temperature overnight. The product was twice recrystallized from approximately 150 ml of hexane and vacuum dried. The yield was approximately 75% with a slight enrichment of the *para*-isomer (*meta*/*para* ratio of ca. 45/55). ^{1}H n.m.r. ($CDCl_3$), δ 8.30 and 7.92 (d, 1H$_1$, *meta*-Ar-H), 8.10 (s, 1H, *para*-Ar-H), δ 4.50–4.38 (q, 4H, methylene), 1.39–1.36 (t, 6H, methyl).

Aminobenzoate terminated poly(propylene oxide). Aminobenzoate terminated oligo(propylene oxide)s were prepared according to the procedure of Hedrick *et al.*[27]. Hydroxyl terminated oligomers (5000 and 10 000 g mol^{-1} nominal molecular weights) were reacted with a five-fold excess of 4-nitrobenzoyl chloride to generate an aromatic nitro end group. The excess nitrobenzoyl chloride was removed by stirring over potassium carbonate. Reduction of the nitro terminated oligomers with Pearlman's catalyst gave clean amine terminated oligomers with molecular weights of 3500 and 6500 g mol^{-1} as determined by ^{1}H n.m.r. and by titration.

Aminophenyl carbonate terminated poly(propylene oxide). The aminophenyl carbonate terminated propylene oxide oligomers were prepared by reacting a five-fold excess of nitrophenyl chloroformate with hydroxy terminated propylene oxide oligomers (5000 and 10 000 g mol^{-1} nominal molecular weight) in tetrahydrofuran (THF) using pyridine as an acid acceptor[27]. After several hours, the insoluble amine hydrochloride salt and nitrophenyl chloroformate complex were removed by filtration and the mother liquor was reduced with Pearlman's catalyst. After reduction the oligomer was subjected to the

appropriate washings to remove the remaining amine hydrochloride salts. This procedure afforded 2300 and 5600 g mol^{-1} oligomers as determined by ^{1}H n.m.r. and potentiometric titration.

3,5-Diaminobenzoate terminated poly(propylene oxide). A 50 ml flask was charged with 20.0 g (8.65 mmol OH) of OH terminated poly(propylene oxide) which had been dried by azeotroping the neat liquid with toluene and subsequently stripping the toluene in a Kugelrohr at 125–150°C at 20 μm pressure. Next, 0.911 g (9 mmol) of dry triethylamine was added, followed by 2.006 g (8.7 mmol) of distilled dinitrobenzoyl chloride. The reaction mixture was stirred overnight and then diluted with 25 ml of diethyl ether. The precipitated triethylamine salt was then filtered, washed with an additional 50 ml of diethyl ether, and the combined filtrates concentrated on the rotary evaporator. The amorphous residue was then taken up in ca. 50 ml of ethyl acetate, 150 mg of $Pd(OH)_2$ on activated carbon was added and the mixture reduced with hydrogen at ~1 atm for 48 h. Once hydrogen absorption had ceased, the mixture was filtered through a bed of celite and activated charcoal and the ethyl acetate solution evaporated. The resulting diamino derivative was again azeotroped with toluene to facilitate drying. The excess toluene was then distilled from the flask and finally with a Kugelrohr at 125°C (20 μm) to remove residual toluene. This yielded the diamino terminated propylene oxide oligomers as clear, brownish liquids with molecular weights of 3400 and 7900 g mol^{-1}, respectively.

Polymerizations

Triblock copolymers were prepared in a two-stage process which included the poly(amic acid) formation followed by imidization. First, the amino functional propylene oxide oligomer (0.25 g, 0.0000446 mol) and FDA (0.4119 g, 0.00118 mol) were charged into a flask together with the solvent, NMP (10 ml). The ODPA (0.3737 g, 0.0011 mol) was later added to the solution at 5°C, yielding the target poly(amic acid) in 24 h. Imidization of the poly(amic acid) was accomplished either thermally with a dehydrating cosolvent (i.e. CHP) or chemically with an acetic anhydride/pyridine mixture. For the case of chemical imidization, excess acetic anhydride (0.2952 g, 0.00289 mol) and pyridine (0.2287 g, 0.00289 mol) were added and slowly heated to 90°C and held for 6–8 h. The resulting polymers were precipitated in methanol and heated (80°C) in a vacuum oven for 24 h. For the case of thermal imidization, CHP was used together with NMP as a cosolvent (50/50 vol%), since CHP is not miscible with water above ~80°C, thus effectively dehydrating the system. Imidization was accomplished by heating the polymerization to 180°C (24 h) according to a procedure developed by McGrath and co-workers[30]. The resulting polymers were isolated in a water/methanol mixture, rinsed with isopropanol and dried in a vacuum oven (50°C).

The amic ester propylene oxide triblock copolymers were prepared by the co-reaction of the amino terminated propylene oxide oligomers with FDA and PMDA diethyl ester diacyl chloride in NMP in the presence of *N*-methylmorpholine. A detailed procedure designed to prepare an amic ester propylene oxide copolymer with a propylene oxide oligomer of 5600 g mol^{-1} molecular weight with 25 wt% propylene oxide composition is provided. A three-necked flask equipped with an overhead stirrer and addition funnel was charged with propylene oxide oligomer **1b** (0.25 g, 0.00007143 mol), FDA (0.4801 g, 0.001378 mol), and carefully rinsed in with 20 ml of NMP. Throughout the polymerization N_2 was passed through the system. The solution was then cooled to −5°C, and *N*-methylmorpholine (0.316 g, 0.003124 mol) was added to the solution. The PMDA diethyl ester diacyl chloride (0.4907 g, 0.00141 mol) was dissolved in ~25 ml of methylene chloride, and added in increments over a 2 h period so as to slowly approach the stoichiometric end point. The polymerizations were allowed to proceed overnight, and isolated by precipitation in methanol/water, rinsed with water (to remove excess salts) and subjected to an isopropanol rinse (to remove possible homopolymer contamination), and dried in a vacuum oven.

The graft copolymers derived from ODPA with FDA were prepared via the poly(amic acid) route followed by chemical imidization. The diamino functional propylene oxide oligomer (0.75 g, 0.000217 mol) and FDA (1.1834 g, 0.00339 mol) were charged into the flask and dissolved in 15 ml of NMP. The solution was allowed to cool to 5°C and the ODPA (1.121 g, 0.00361 mol) was added. Stirring the solution for 24 h yielded the target poly(amic acid). Imidization was carried out chemically with acetic anhydride/pyridine (0.6872 g, 0.00869 mol) mixture at 90°C for 6–8 h. The copolymers were isolated by precipitation in a mixture of methanol/water (20/80 v/v) and washed in isopropanol for 1 h at room temperature. The copolymers were then dried in a vacuum oven (80°C) for 24 h.

The amic ester poly(propylene oxide) graft copolymers were prepared by the polymerization of the diamino functional propylene oxide oligomer and FDA with the PMDA diethyl ester diacyl chloride. A detailed procedure designed to prepare an amic ester propylene oxide graft copolymer from a propylene oxide oligomer **1d** is provided. A three-necked flask equipped with an overhead stirrer and an additional funnel was charged with propylene oxide (0.25 g, 7.24×10^{-5} mol), FDA (0.4673 g, 0.00134 mol) and 10 ml of NMP. The solution was cooled to 5°C and *N*-methylmorpholine (0.3156 g, 0.00312 mol) was added to the solution. The PMDA diester diacyl chloride (0.4907 g, 0.00141 mol) was dissolved in ~10 ml of methylene chloride, and added drop by drop over a 2 h period. The polymerizations were allowed to proceed overnight and were carried out under dry nitrogen. The polymers were recovered by precipitation in methanol/water (20/80 v/v) and rinsed with isopropanol for 1 h at room temperature. The copolymers were dried under vacuum at 80°C.

Foam formation

The copolymers were dissolved in NMP at a concentration of 9–15% solids. Coatings of 10–25 μm in thickness were obtained by spin coating at 2000 rev min^{-1} on 2.54 cm diameter Si wafers or by doctor blading. The removal of the solvent and imidization, if required, were accomplished by heating the polymer films to 300°C at 5°C min^{-1} and maintaining them at 300°C for 1.0 h in a nitrogen atmosphere. The films were then cooled to room temperature and reheated to 240°C at a rate of 5°C min^{-1} and maintained at 240°C for 6–8 h in air.

Characterization

Glass transition temperatures, taken as the midpoint of the change in the slope of the baseline, were measured on a DuPont 1090 instrument at a heating rate of $10°C\,min^{-1}$. A Polymer Laboratories' Dynamic Mechanical Thermal Analyzer operating at 10 Hz with a heating rate of $10°C\,min^{-1}$ in the tension mode was used to assess the dynamic mechanical properties. Isothermal and variable temperature ($5°C\,min^{-1}$ heating rate) thermal gravimetric analysis (t.g.a.) measurements were performed on a Perkin-Elmer model TGA-7 instrument in a nitrogen atmosphere. Density measurements were obtained with a density gradient column composed of water and calcium nitrate. The column was calibrated against a set of beads of known densities at 25°C. At least two specimens were used for each density measurement.

Small-angle X-ray scattering studies were performed on Beamline I-4 at the Stanford Synchrotron Radiation Laboratory. Details of the beamline optics are described elsewhere[29]. In these experiments, X-rays of wavelength 1.53 Å were passed through a Mettler FP85 hot stage where the sample was mounted. X-ray scattering profiles were obtained either as the sample temperature was ramped at $10°C\,min^{-1}$ or at a specific temperature as a function of time. Experiments were performed under a steady flow of N_2 or in air. Samples of ~0.25 mm in thickness were prepared by placing stacks of thin films in a sample cell with Kapton windows. Standard procedures were used to correct the scattering profiles for parasitic scattering, electronic noise and sample absorption. Scattering profiles will be presented as a function of the scattering vector, Q, which is given by $(4\pi/\lambda)\sin\theta$, where λ is the wavelength and 2θ is the scattering angle.

RESULTS AND DISCUSSION

Two synthetic approaches were surveyed to implement the block copolymer strategy as a route to polyimide nanofoams. Since ODPA/FDA polyimide is soluble in the fully imidized form, these block copolymers were prepared by a two-stage process, which included the poly(amic acid) formation followed by imidization (*Scheme 1*). This solubility permits the characterization of the polymer as well as the processing and foaming conditions surveyed. The poly(amic alkyl ester), on the other hand, was employed as a soluble precursor to the PMDA/FDA based copolymers, since these structures are not soluble in the fully imidized form (*Scheme 2*). This scheme allows for the isolation and characterization of a processable form of the copolymer.

One criterion for the thermally decomposable coblock is the preparation of well-defined functional oligomers. This block must also decompose quantitatively into non-reactive species that can readily diffuse through a glassy polyimide matrix. The temperature at which decomposition occurs is crucial. The decomposition temperature must be sufficiently high to permit standard film preparation and solvent removal yet be well below the T_g of the polyimide block to avoid foam collapse. Thus, the temperature difference between the decomposition temperature of the labile block and the T_g of the high temperature polymer matrix defines the 'processing window'. The thermally decomposable coblock used for this study was poly(propylene oxide), since it decomposes well below the T_gs of the polyimides. In fact, significant latitude is afforded by the use of poly(propylene oxide) as the labile component, since it is stable to temperatures as high as 300°C in an inert atmosphere, allowing solvent removal and imidization if necessary. In the presence of oxygen, the decomposition temperature drops dramatically (~200°C), such that temperatures well below T_g of many polyimides can be used to facilitate the foaming process. This variable decomposition temperature allows for a greatly enhanced processing window for processing and subsequent foam formation.

Monofunctional hydroxyl terminated propylene oxide oligomers were converted into either the monoamino or

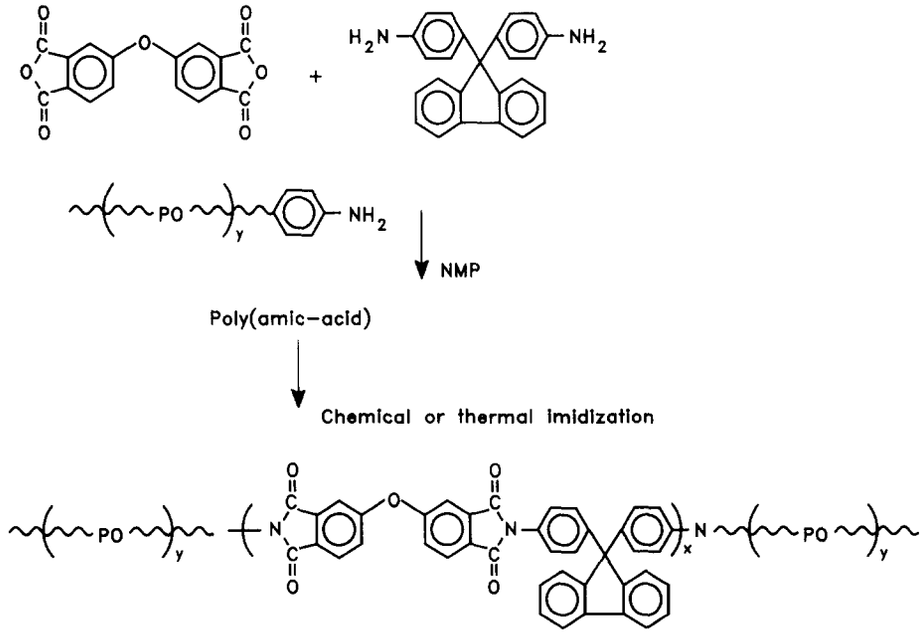

Scheme 1

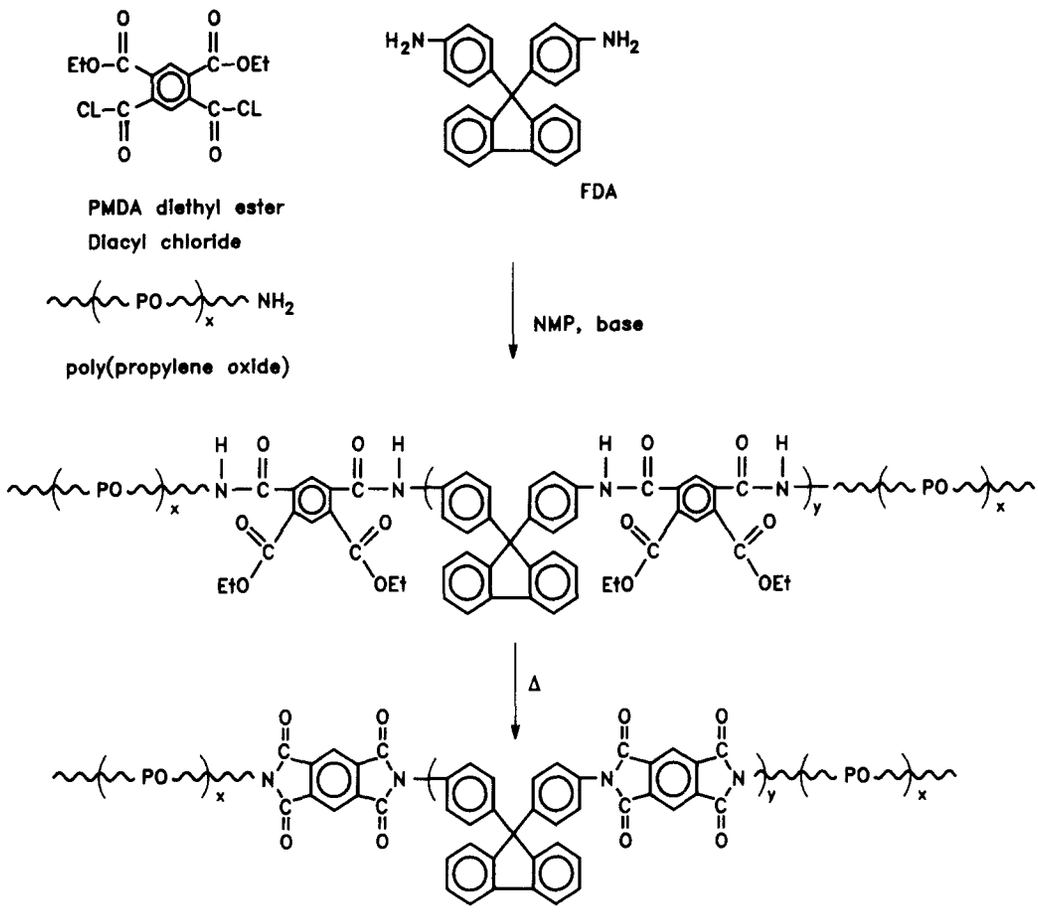

Scheme 2

diamino functionalities suitable for the copolymerization to enable copolymers of either triblock or graft architectures, respectively. Use of the preformed monofunctional amine terminated propylene oxide oligomers afforded an ABA triblock architecture, where the propylene oxide component terminated the growing polyimide chains. The average molecular weight of the propylene oxide blocks is identical to that of the preformed oligomers, whereas the molecular weight of the imide block was controlled by the stoichiometric imbalance between the dianhydride and diamine which is governed by the block length, functionality and composition of the propylene oxide. Conversely, the graft system, prepared from a propylene oxide oligomer where one end contains an aromatic diamine, should be particularly advantageous since this decouples the molecular weight of the polyimide component of the copolymer from the composition and molecular weight of the propylene oxide block.

Two approaches were developed by Hedrick *et al.*[26,27] to transform the hydroxyl end group of the propylene oxide oligomers to an aromatic monofunctional amine including an aminobenzoate and aminophenyl carbonate end functionalities. The aminophenyl carbonate end-capped propylene oxide oligomers were prepared by the reaction of the monohydroxyl terminated propylene oxide oligomers with 4-nitrophenyl chloroformate in methylene chloride containing pyridine as an acid acceptor. This was reduced with Pearlman's catalyst and hydrogen to the corresponding amine. The second approach involved coupling the hydroxyl terminated oligomers with 4-nitrobenzoyl chloride, followed by reduction with the Pearlman's catalyst with hydrogen to yield the aminobenzoate end group. The diamino functionalized propylene oxide oligomer was prepared in an analogous manner. The monohydroxyl functional propylene oxide oligomers were derivatized with 3,5'-dinitrobenzoyl chloride and then reduced with Pearlman's catalyst and hydrogen to the target diamine (*Scheme 3*). Two monohydroxyl propylene oxide oligomers with nominal molecular weights of 5000 and 10000 g mol^{-1} were derivatized. The characteristics of these oligomers and the derivatized oligomers are shown in *Table 1*. The molecular weights were determined by both ^{1}H n.m.r. and titration measurements. The discrepancy in the molecular weights of the functionalized oligomers is believed to result from the work-up procedure involved during the derivatizations.

Table 1 Characteristics of propylene oxide oligomers

Sample	Terminal functional group	Molecular weight (g mol^{-1})[a]
1a	aminophenyl carbonate	2300
1b	aminophenyl carbonate	5600
1c	aminobenzoate	3500
1d	aminobenzoate	6500
1e	diaminobenzoate	3100
1f	diaminobenzoate	7900

[a] Determined by ^{1}H n.m.r. and titration measurements

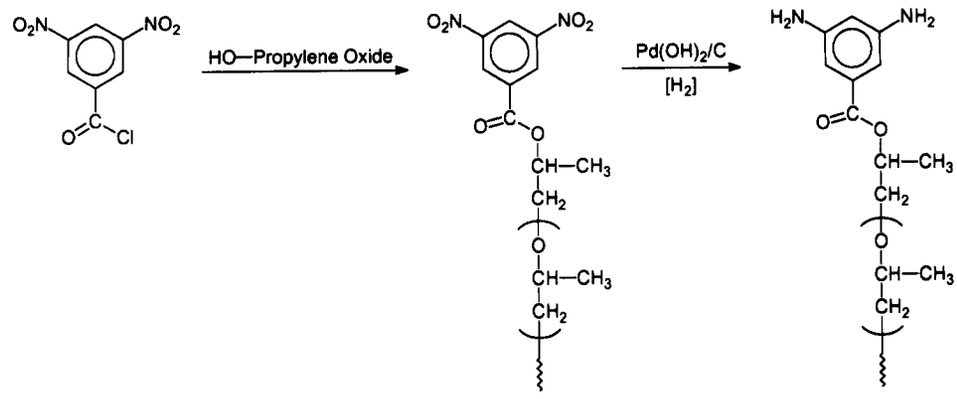

Scheme 3

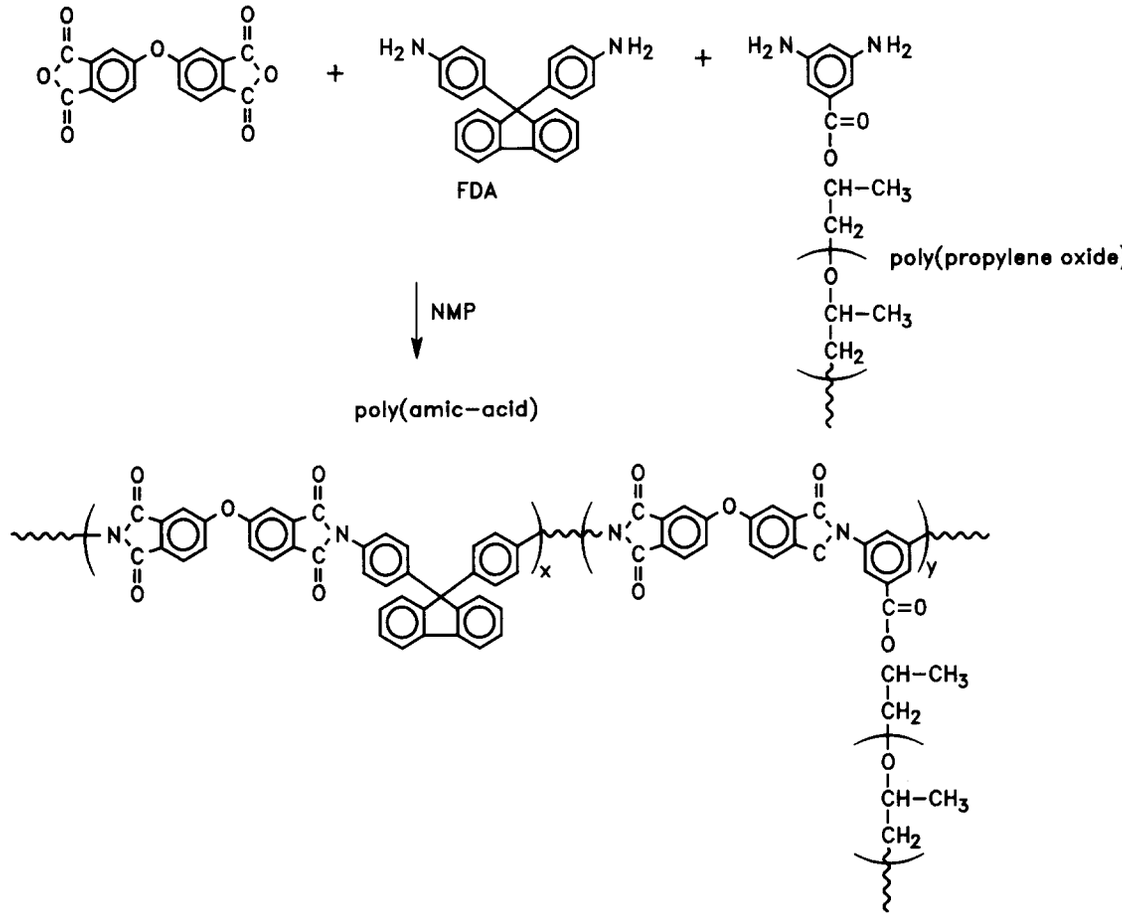

Scheme 4

Due to the solubility of the ODPA/FDA polyimide, the ODPA/FDA imide–propylene oxide copolymers were prepared via the poly(amic acid) precursor route followed by imidization. Both triblock (*Scheme 1*) and graft (*Scheme 4*) molecular architectures were surveyed as a means of obtaining well-defined copolymers. The architecture depended on the functionality of the propylene oxide oligomer used in the synthesis (i.e. mono- or difunctional). In addition, in this study propylene oxide oligomers with both the aminobenzoate and aminophenyl carbonate terminal end groups were investigated. The copolymers derived from the aminobenzoate terminal propylene oxide oligomers showed low propylene oxide incorporation and significant homopolymer (polyimide) contamination. Presumably this amino functionality is sufficiently deactivated under the standard polymerization conditions used to limit the propylene oxide incorporation. Conversely, the copolymers derived from the aminophenyl carbonate terminated propylene oxide oligomers showed the expected propylene oxide incorporation. In this latter case, the synthesis involved the incremental addition of solid ODPA to a solution of FDA and either the monofunctional or difunctional propylene oxide oligomer. The polymerizations were mediated in NMP

at solid compositions of approximately 10–12 wt%. The polymerizations were maintained at room temperature for 24 h yielding viscous solutions of the target poly(amic acid)s. Imidization of the poly(amic acid) solutions was carried out directly and was accomplished either thermally or chemically. Chemical imidization was achieved with excess acetic anhydride and pyridine in 6–8 h at 100°C, whereas the thermal imidization was performed in solution at 185°C (24 h) with CHP as a cosolvent to effect the dehydration[30].

The insolubility of the PMDA/FDA polyimide required an alternative route to well-defined block copolymers. Therefore, the poly(amic alkyl ester) was employed as the soluble precursor to the polyimide[28]. The poly(amic alkyl ester) precursor route to polyimide copolymers allows more synthetic flexibility than the poly(amic acid) analogue since the former is soluble in a variety of solvents and solvent mixtures. This permits the synthesis of copolymers with greater structural variety in the backbone as well as in the coblock type, length and composition. The hydrolytically stable poly(amic alkyl ester) precursors may be isolated, characterized and washed to remove possible homopolymer contamination prior to imide formation[28]. Furthermore, the poly(amic alkyl ester) route may be advantageous since imidization occurs at higher temperatures, which imparts more mobility to the polymer and hence favours a morphology closer to the equilibrium structure. The synthesis involved the incremental addition of PMDA diethyl ester diacyl chloride in methylene chloride to a solution of either monofunctional or difunctional propylene oxide oligomers and FDA in NMP containing pyridine as the acid acceptor, to yield triblock (*Scheme 2*) or graft (*Scheme 5*) molecular architectures. Due to the enhanced reactivity of the acid chloride in this synthetic approach, both the aminophenyl carbonate and the aminobenzoate terminated propylene oxide oligomers were successfully incorporated into the copolymer. The solids compositions were maintained at approximately 15 wt% for each polymerization. Completion or near-completion of the

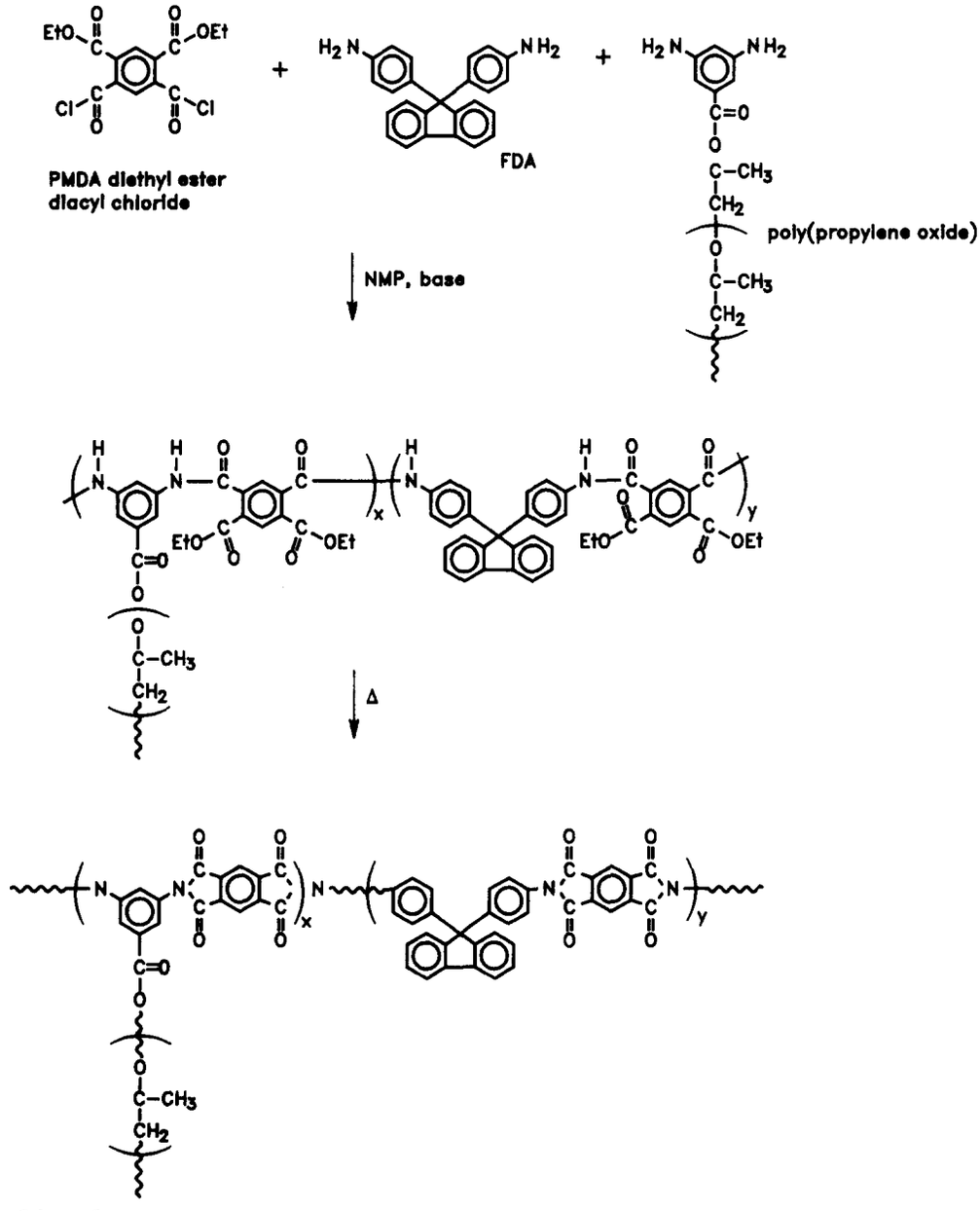

Scheme 5

Table 2 Characteristics of imide–propylene oxide copolymers

Sample	Propylene oxide block	Polyimide block type	Molecular architecture	Propylene oxide composition (wt%)			Calculated polyimide mol. wt. ($g\,mol^{-1}$)
				Charge	^{1}H n.m.r.	t.g.a.	
2	**1a**	ODPA/FDA	triblock	15	10.8	10.4	13000
3	**1a**	ODPA/FDA	triblock	25	18.7	16.5	6900
4	**1b**	ODPA/FDA	triblock	15	13.1	13.0	31700
5	**1b**	ODPA/FDA	triblock	25	22.5	22.5	16800
6	**1c**	ODPA/FDA	graft	25	24	24	–[a]
7	**1f**	ODPA/FDA	graft	25	15.6	16	–[a]
8	**1a**	PMDA/FDA	triblock	15	12.6	8.8	19800
9	**1a**	PMDA/FDA	triblock	25	20.4	18.4	10500
10	**1b**	PMDA/FDA	triblock	15	14.3	9.2	36800
11	**1b**	PMDA/FDA	triblock	25	22.0	18.4	19500
12	**1c**	PMDA/FDA	graft	15	12.3	11	–[a]
13	**1c**	PMDA/FDA	graft	25	19.8	20	–[a]
14	**1f**	PMDA/FDA	graft	15	7.5	–	–[a]
15	**1f**	PMDA/FDA	graft	25	12.8	–	–[a]

[a] Graft copolymers are prepared with 1:1 stoichiometry of amine to anhydride

polymerization was taken as the point where the viscosity increased dramatically. The copolymers were isolated in a methanol/water mixture, washed with water to remove remaining salts, rinsed with methanol to remove possible poly(propylene oxide) homopolymer and dried at 50°C (24 h) under vacuum.

A number of imide–propylene oxide copolymers were prepared (**2–15**) derived from ODPA/FDA (**2–7**) and PMDA/FDA (**8–15**) polyimide blocks of both graft (**6**, **7** and **12–15**) and triblock (**2–5** and **8–11**) architectures (*Table 2*). Two propylene oxide block lengths with compositions of 15 and 25 wt% were investigated, as denoted in *Table 2*. The propylene oxide compositions in the copolymer were deliberately maintained low. It was anticipated that a propylene oxide composition of 15 wt% would, in principle, produce discrete domains of the thermally labile component in a high temperature polymer matrix, while the higher propylene oxide composition would approach cylindrical or more interconnected types of structure. The composition of propylene oxide in the copolymer was assessed by both ^{1}H n.m.r., by comparison of the integrated polyimide signal to that of the propylene oxide resonances, and t.g.a., by measuring the weight retention after decomposition of the thermally labile block. For the triblock copolymers derived from ODPA/FDA polyimide (**2–5**), the propylene oxide incorporated into the copolymer was somewhat lower than that charged, which was, most likely, due to the solvent rinses which removed propylene oxide rich copolymer. However, the propylene oxide incorporation in the ODPA/FDA polyimide based graft copolymers (**6**, **7**) was significantly lower than the charge. This results from the enhanced solubility of the copolymer in the precipitation solvent due to the higher propylene oxide block length. The propylene oxide incorporated into the PMDA/FDA based poly(amic ester) triblock copolymers agreed more closely with the initial monomer charge. However, as in the previous case, the propylene oxide incorporation in the graft system was considerably lower, particularly for the higher propylene oxide block length. The average molecular weight of the propylene oxide block is identical to that of the preformed oligomers, while the molecular weight of the imide block was controlled by the stoichiometric imbalance between ODPA and FDA or PMDA and FDA, dictated by the propylene oxide block length, functionality and composition. This can be critical when low molecular weight propylene oxide block lengths are employed. The calculated number average molecular weights of the polyimide blocks based on the monomer offset are shown in *Table 2*. The incorporation of lower propylene oxide block lengths produced low molecular weight polyimide blocks, which may deleteriously affect the T_g, mechanical properties, morphology and the processing window for foam formation. The molecular weight of the imide block in the graft systems should be decoupled from the propylene oxide block length or composition since there are no monofunctional or chain terminating monomers/oligomers. The molecular weight of the propylene oxide graft in these systems should be identical to the molecular weight of the preformed oligomer.

The processing window for film and foam formation was primarily established with the imide–propylene oxide copolymers derived from ODPA/FDA, since these copolymers are soluble in the imide form and may be isolated and characterized at various stages of the processing. It is critical that the decomposition of the labile block should occur substantially below the T_g of the polymer matrix. Furthermore, the casting solvent must be effectively removed, without propylene oxide degradation, to minimize plasticization of the polyimide matrix, which would further narrow the processing window. Samples were cast from NMP, cured, and the processing window for film and foam formation was established by ^{1}H n.m.r., t.g.a. and dynamic mechanical measurements. Since poly(propylene oxide) is stable to 300°C in nitrogen, samples cured to this temperature to remove the casting solvent should retain their propylene oxide compositions. Shown in *Figure 1* are the ^{1}H n.m.r. spectra for a copolymer cured in nitrogen at 220, 260

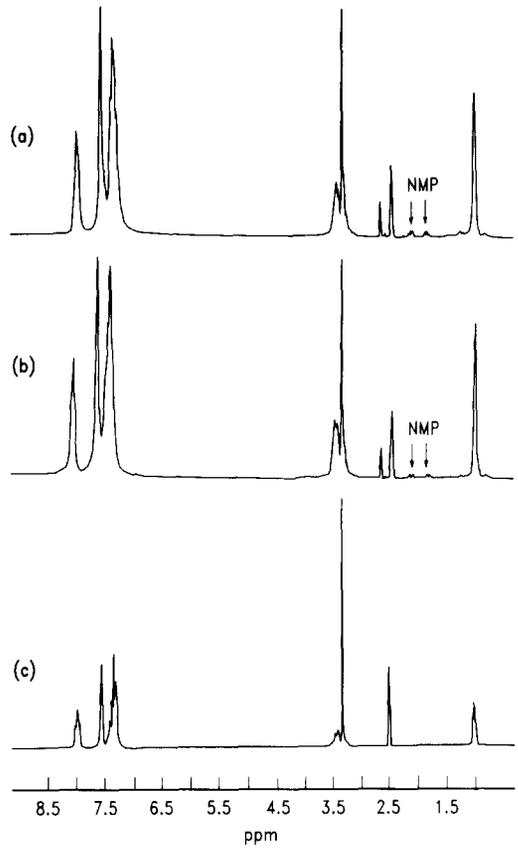

Figure 1 ^{1}H n.m.r. spectra of copolymer **2** after curing at (a) 220°C, (b) 260°C and (c) 300°C

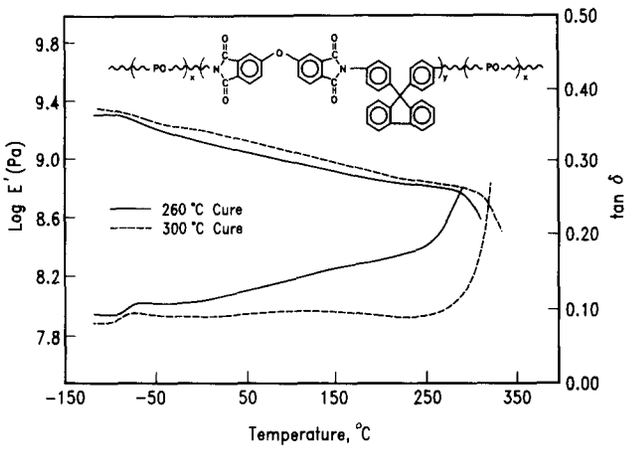

Figure 2 Dynamic mechanical spectra of copolymer **2** after curing to 260 and 300°C

and 300°C. Regardless of the cure temperature, the propylene oxide composition is retained. The spectra of samples cured at 220 and 260°C clearly show the retention of ~1–3 wt% of the casting solvent (NMP) in the film, while the sample cured at 300°C showed no detectable signs of NMP. The dynamic mechanical analysis showed different behaviour depending on the cure temperature up to a temperature of 300°C (*Figure 2*). Cure temperatures of 300°C and above show no change in the position of the polyimide T_g. However, a 20–40°C depression in T_g of the polyimide block is observed at cure temperatures below 300°C, presumably resulting from plasticization by the residual NMP. For our experiments, films of the copolymer were cast and cured under nitrogen to 300°C for 1 h to afford clear, tough films.

The imide–propylene oxide copolymer with an imide block derived from PMDA/FDA required imidization of the poly(amic alkyl ester) precursor form. Volksen and co-workers found that the temperature range over which imidization occurred for the poly(amic ethyl ester) derived from PMDA/ODA was from 240 to 355°C, with a maximum in the rate at 255°C[28]. For our experiments, the imidization temperature was restricted by the propylene oxide decomposition temperature. The processing conditions used for these copolymers were the same as those described for the ODPA/FDA based copolymers, since 300°C for 1 h appears to be near the time and temperature limit of quantitative propylene oxide retention. Samples were cast from NMP and cured at 300°C for 1 h to remove the casting solvent and effect imidization. I.r. and calorimetry measurements indicated that the imidization was essentially quantitative, with minimal loss to the propylene oxide composition as measured by t.g.a. Furthermore, samples prepared in this manner showed an imide T_g in excess of 500°C, suggesting near-quantitative imidization.

The dynamic mechanical results for the imide–propylene oxide triblock copolymers with an imide block derived from ODPA/FDA are shown in *Figures 3* and *4*. The copolymers (**2–5**) exhibited two transitions, characteristics of a microphase-separated morphology. The transition occurring near −60°C is similar to that seen for the propylene oxide oligomers (**1c** and **1d**). The copolymers containing the lower block lengths showed damping peaks which are rather diffuse and broad, which suggests that the phases are not pure. The copolymers with the higher propylene oxide block length showed sharp damping peaks, in most cases, indicating that the phases are pure and phase boundaries are sharp. Similar effects were seen with the imide transition, where the copolymers containing the lower molecular weight propylene oxide block showed a depression in the T_g of the imide phase, whereas with the higher molecular weight propylene oxide block no depression was seen. Any depression in the T_g of the imide phase narrows the processing window for foam formation. For the ODPA/FDA polyimide based graft copolymers, a similar behaviour (*Figure 5*) was observed.

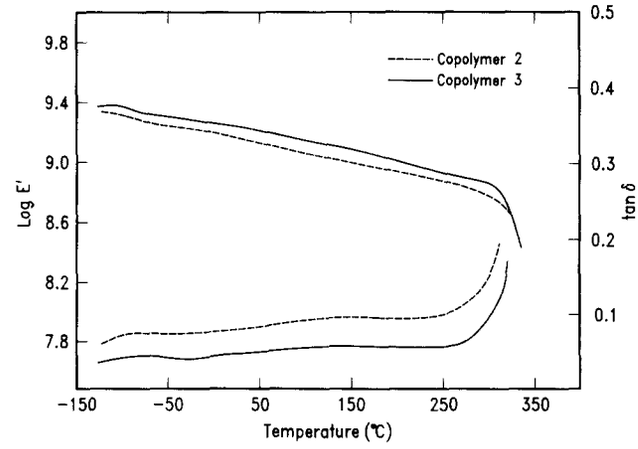

Figure 3 Dynamic mechanical spectra for copolymers **2** and **3**

The dynamic mechanical results for the imide–propylene oxide triblock copolymers derived from PMDA/FDA are shown in *Figures 6–9*. As for the ODPA/FDA based copolymers, two transitions characteristic of a microphase-separated morphology were seen. The transition occurring near −60°C is nearly identical to that of the propylene oxide oligomer used in the synthesis. However, the damping peak and drop in modulus are associated with the propylene oxide transition, suggestive of a diffuse phase boundary. In each case, the modulus above the propylene oxide transition is essentially constant, which is in keeping with the dynamic mechanical spectrum of the PMDA/FDA homopolymer. In these copolymers, there was no evidence of phase mixing within the polyimide phase.

The generation of the nanofoam was accomplished by subjecting the copolymer films to a thermal treatment in air to decompose the propylene oxide. Due to the rather narrow processing window of the ODPA/FDA based copolymers, mild temperatures were employed to decompose the propylene oxide block. Furthermore, if the degradation of the propylene oxide block is considerably

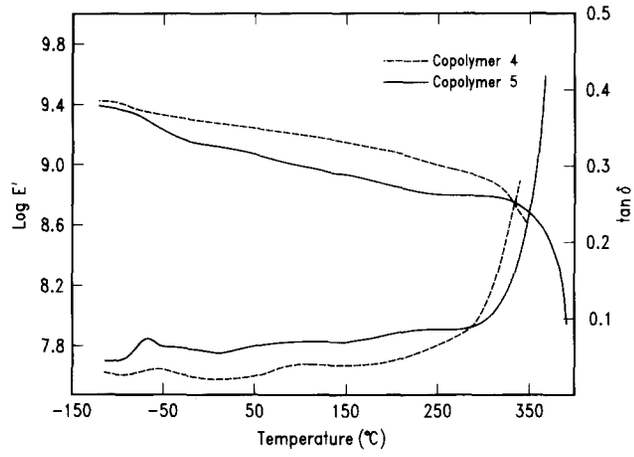

Figure 4 Dynamic mechanical spectra for copolymers **4** and **5**

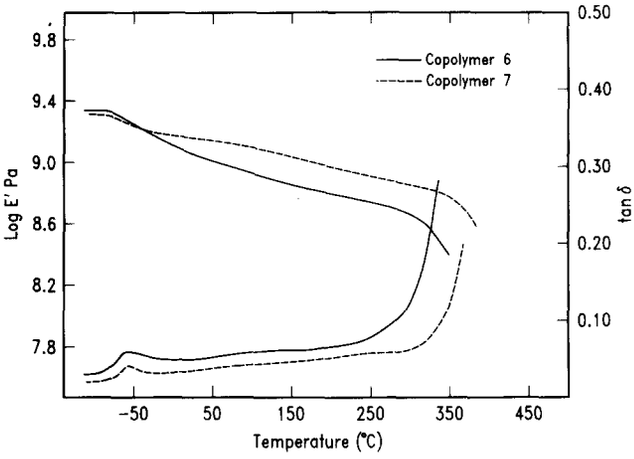

Figure 5 Dynamic mechanical spectra for copolymers **6** and **7**

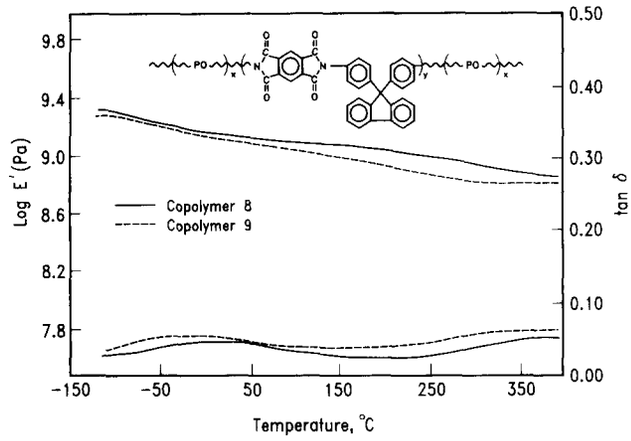

Figure 6 Dynamic mechanical spectra for copolymers **8** and **9**

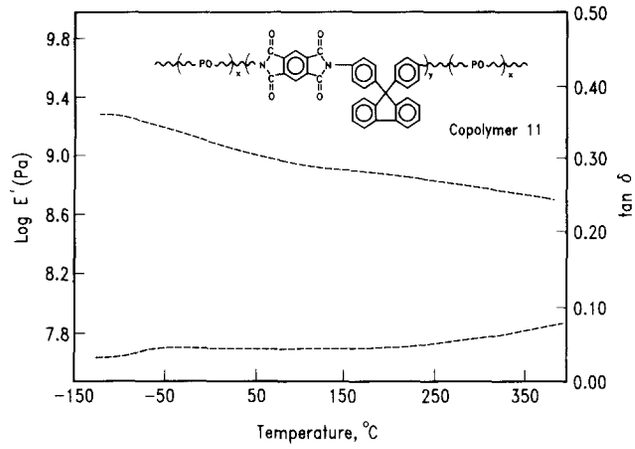

Figure 7 Dynamic mechanical spectra for copolymer **11**

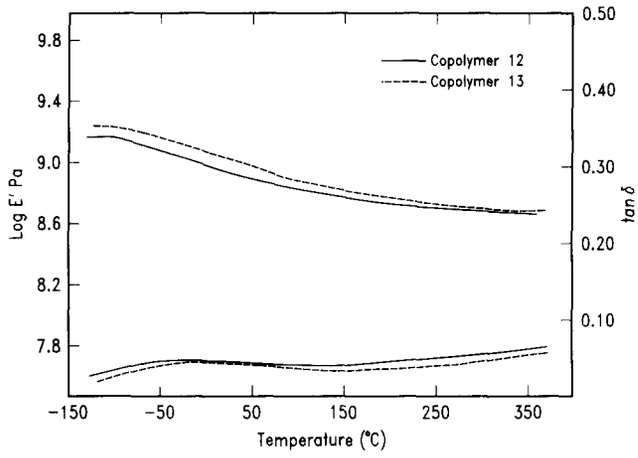

Figure 8 Dynamic mechanical spectra for copolymers **12** and **13**

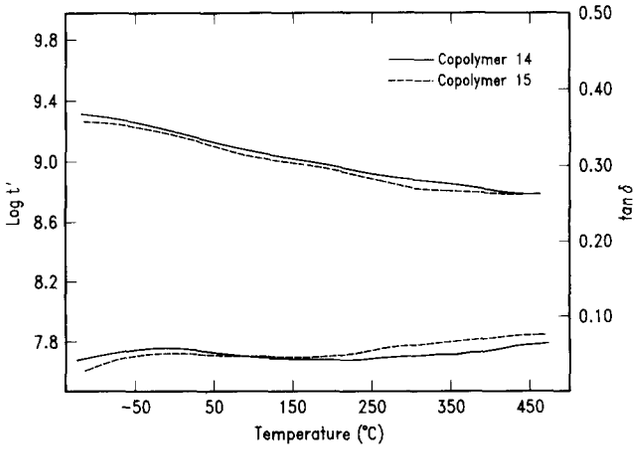

Figure 9 Dynamic mechanical spectra for copolymers **14** and **15**

faster than the diffusion of the low molecular weight by-product, plasticization of the polyimide block could occur which would lead to foam collapse. This effect should also be minimized by the lower decomposition temperature. Foam formation was accomplished by heating the copolymer at 240°C in air for 15 h. Shown in *Figure 10* are plots of the isothermal weight loss as a function of time for copolymers **3**, **4** and **11**, which clearly show, in each case, the quantitative decomposition of the propylene oxide component. Once subjected to this treatment, the sample was redissolved and characterized. *Figure 11* shows the ^{1}H n.m.r. spectrum of the foamed sample with less than 1% of the propylene oxide coblock remaining as compared to the neat ODPA/FDA polyimide homopolymer. There was no evidence of residual by-products of the degradation nor of chemical modification of the polyimide block. Conversely, higher temperatures for foam formation were allowed for the imide–propylene oxide copolymers comprising the PMDA/FDA imide block, due to the substantially higher T_g. Foam formation was achieved by heating the copolymer at 240°C for 10 h or at 300°C for 2 h.

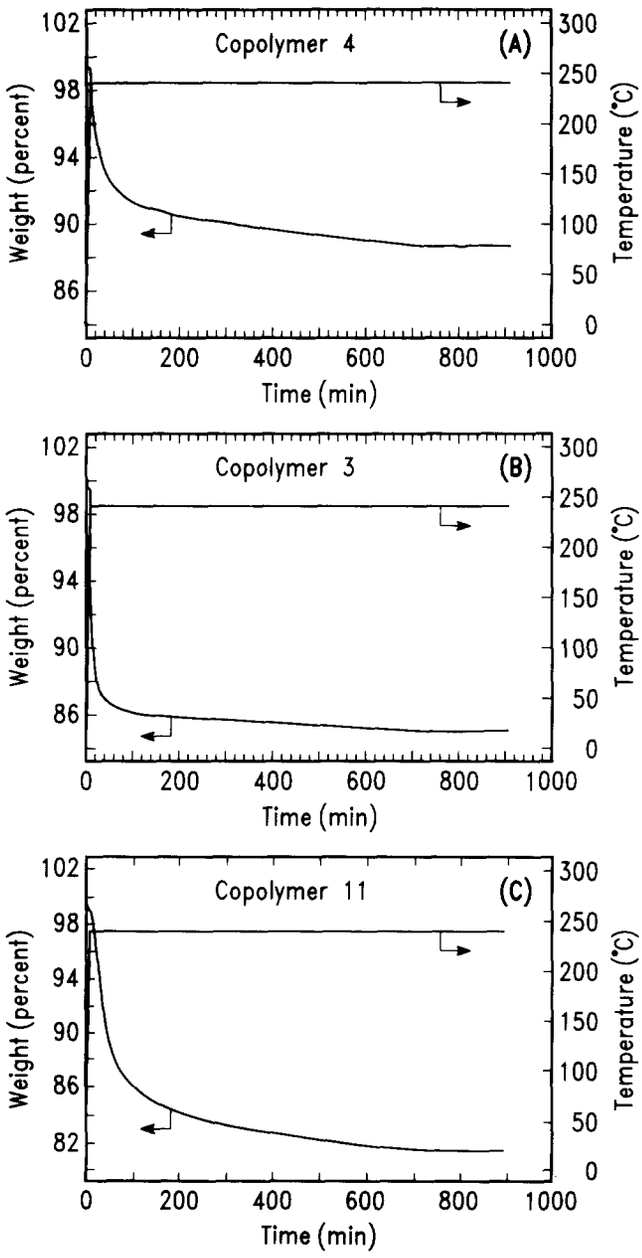

Figure 10 Isothermal t.g.a. thermograms for copolymers **3**, **4** and **11** at 240°C in air

The density of the polymer clearly shows the formation of a foamed polymer. The density values of the foamed copolymers together with the polyimide homopolymers are shown in *Table 3*. The density values for the ODPA/FDA and PMDA/FDA polyimides were both 1.28 g cm^{-3}, while most of the copolymers showed substantially lower values. The densities of the foamed copolymers derived from ODPA/FDA ranged from 1.09 to 1.27 g cm^{-3}, which is ~85–99% of that of the polyimide homopolymers. This is consistent with 1–15% of the film being occupied by voids. From these data (i.e. comparison of *Tables 2* and *3*), it appears that the volume fraction of voids or the porosity is substantially less than the volume fraction of propylene oxide in the copolymer (i.e. ~50% or less). Thus, the efficiency of foam formation is poor. Interestingly, the graft copolymer, particularly the one with the low molecular weight propylene oxide block length, showed poorer foam efficiency than the triblock copolymers. These results are surprising since the dynamic mechanical results of the triblock and graft systems appear to be identical with respect to their transitions and 'processing window'.

The density values of the foamed copolymers of PMDA/FDA were ~1–12% less than that of the respective homopolymer. In comparing *Tables 2* and *3*, the foam efficiency for the PMDA/FDA based triblock copolymers is similar to the ODPA/FDA based copolymers (i.e. ~50% or less). The graft copolymers (**12**, **13**) derived from the low molecular weight propylene oxide oligomers essentially collapsed. Conversely, the PMDA/FDA based graft copolymers derived from the high molecular weight propylene oxide block showed substantially higher efficiency in foam formation. This presumably results from the enhanced phase purity with the higher propylene oxide block length, together with the large processing window. Furthermore, the foam structure appears to be stable over a wide temperature range. Shown in *Figure 12* are the densities of the PMDA/FDA based foams held for 1 h at several temperatures. Over the temperature range studied (250–400°C), the density appears to be essentially invariant for the foams derived from the

Table 3 Characteristics of imide foams

Sample	Density (g cm^{-3})	Volume fraction of voids (%)
ODPA/FDA polyimide	1.28	–
PMDA/FDA polyimide	1.28	–
2	1.19	7.0
3	1.09	14.5
4	1.20	6.0
5	–	–
6	1.27	1.0
7	1.16	9.0
8	1.18	8.0
9	1.16	7.2
10	1.17	7.2
11	1.11	12.0
12	1.27	1.0
13	1.24	3.1
14	1.19	5.56
15	1.15	11.0

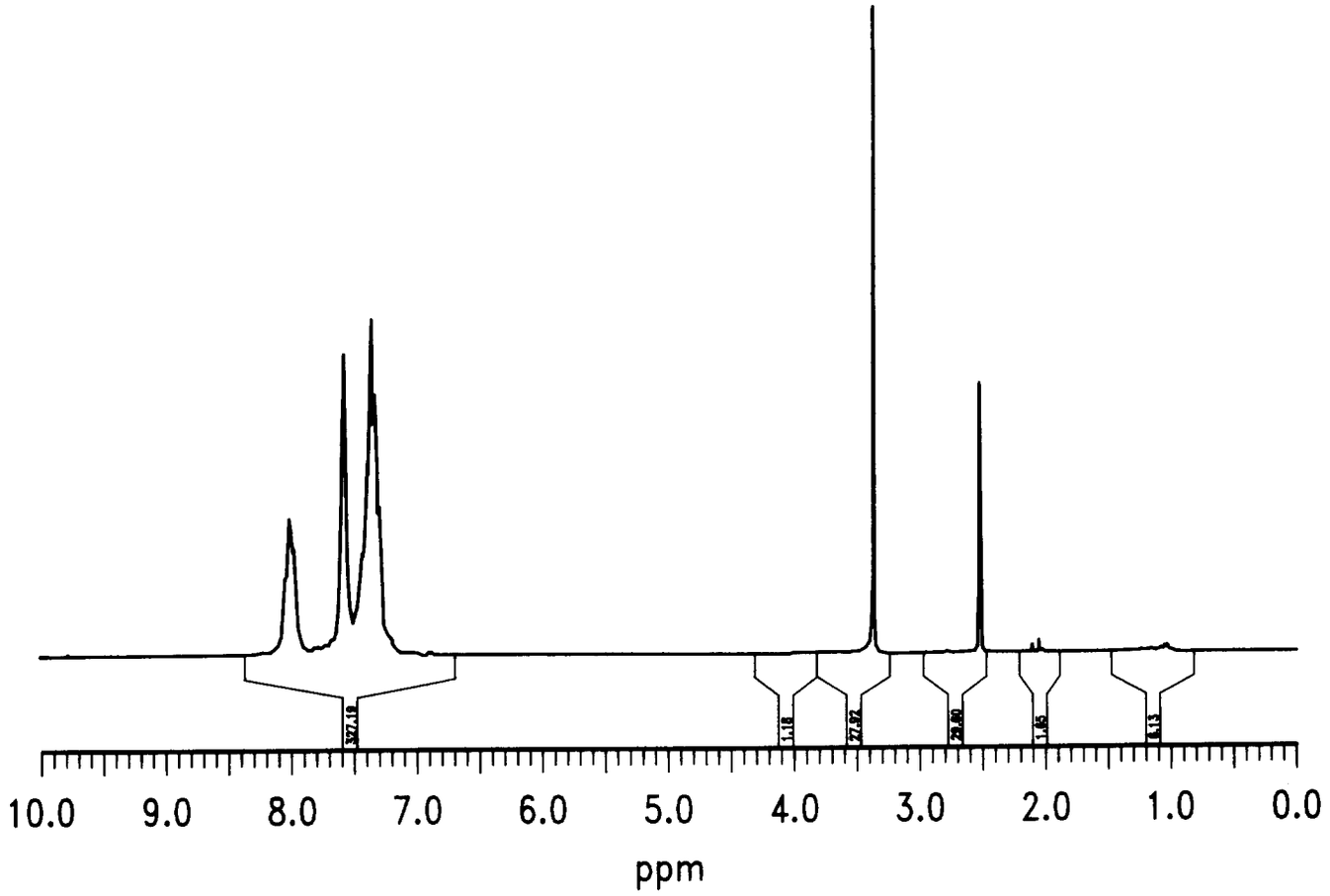

Figure 11 ^{1}H n.m.r. spectrum of copolymer **2** after heating to 240°C for 14 h in air

copolymers with the high molecular weight propylene oxide block. However, the foams derived from the copolymers with the low molecular weight propylene oxide block showed a slight increase in density between 350 and 400°C. Thermal mechanical analysis was also used to study the stability of the cellular structure as a function of temperature. In these experiments, a small tensile deformation was placed on the sample during heating. The deformation is plotted as a function of temperature and the derivative of this plot yields the thermal expansion coefficient. Shown in *Figure 13* is the displacement as a function of temperature for PMDA/FDA and, as expected, the sample expands with temperature up to ~400°C. However, as the temperature approached the T_g or softening point where an increase in the expansion rate is expected, the sample contracted substantially between 400 and 450°C. Over this temperature range some polyimides undergo an ordering which would give rise to a contraction of the film. However, X-ray diffraction studies on both the ODPA/FDA and PMDA/FDA homopolymers showed that the samples were isotropic and underwent no ordering processes. Consequently, this contraction must be associated with residual stress imparted by both the solvent evaporation and imidization. Also shown in *Figure 13* is the thermal mechanical analysis of foamed copolymer **11**. Initially, the foam showed a displacement/temperature profile similar to that of the homopolymer. However, at ~300°C a change in slope is observed, consistent with a minor contraction in the sample. The contraction between 300 and 400°C was calculated to be ~2% (in the plane of

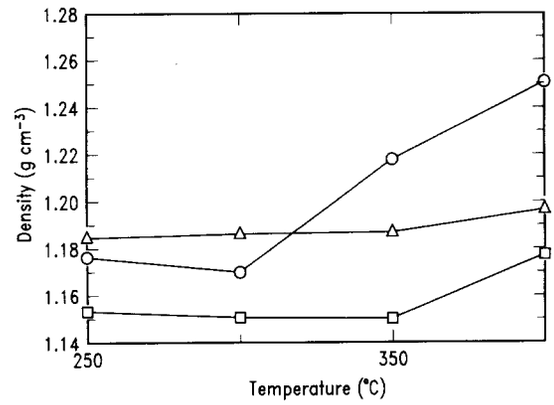

Figure 12 Density as a function of temperature (held at temperature for 1 h) for copolymers **11** (□), **9** (△) and **8** (○)

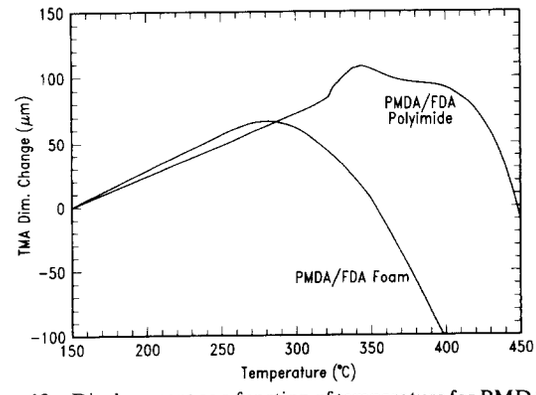

Figure 13 Displacement as a function of temperature for PMDA/FDA polyimide and PMDA/FDA foam from copolymer **11**

the film), which can be correlated with the density measurements as a partial collapse of the foam structure. The foams of ODPA/FDA were stable to 300°C, but the density began to increase at higher temperatures. At 350°C, the density approached that of the homopolymer, indicating that the foam structure had collapsed.

Small-angle X-ray scattering provides a useful means of evaluating the formation of the nanofoam structure due to the length scales probed and the large X-ray contrast between the void and the polymer matrix. Shown in *Figure 14* is the X-ray scattering as a function of the scattering vector, Q, obtained in heating the ODPA/FDA copolymer with propylene oxide from 60 to 250°C at a rate of 5°C min^{-1}. The initial scattering profile showed a peak in the scattering at $Q \simeq 0.017$ Å^{-1}, corresponding to a Bragg spacing of ~367 Å. From the volume fraction of propylene oxide in the copolymer (~0.12), this yields an average size of the propylene oxide domains of ~44 Å. It should be noted that only a single reflection is observed, with no indication of higher order reflections. If the propylene oxide domains were arranged periodically on a lattice, higher order reflections would be expected. Consequently, while the microphase-separated domains are periodic, lattice distortions cause a rapid loss of interferences at higher Q. These distortions arise from two sources. First, the microphase-separated morphology is far from an equilibrium state. Secondly, the size of the propylene oxide domains is polydisperse. The persistence of scattering at much smaller Q also suggests this.

As the sample is heated, the intensity of the scattering increases dramatically and at ~220°C a nearly five-fold increase in the scattering is evident. It should be noted that the scattering increases over the entire scattering vector range but with larger increases being evident at the lower scattering vectors. In addition, the position of the reflection does not change as a function of temperature.

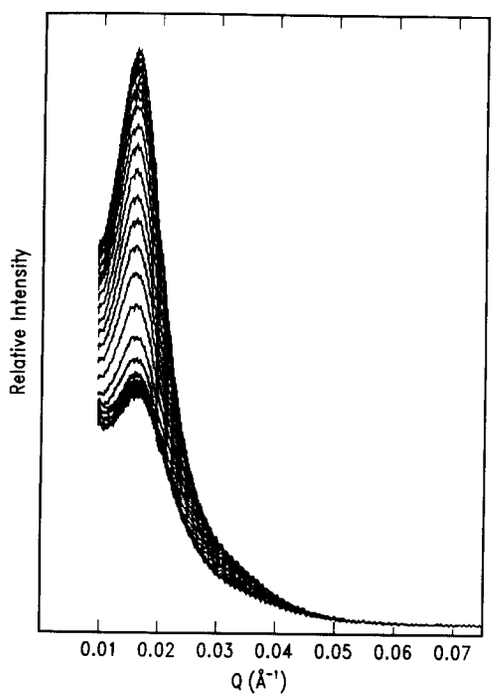

Figure 14 Small-angle X-ray scattering of copolymer **2** as a function of the scattering vector, Q, during heating from 60 to 250°C at 5 C min^{-1}. The scattered intensity is seen to increase with increasing temperature as the propylene oxide block decomposes

Near 220°C the increase in the scattering begins to lessen and an asymptotic value is observed. At first glance, these data indicate that nanofoam formation has been achieved. The increase in the scattering and the invariance of the peak position are precisely the expected result. However, on closer inspection, the scattering data indicate that only partial foam formation has occurred.

In general, the intensity $I(Q)$ of scattering can be written in terms of an interference function, $S(Q)$, and the mean square electron density difference $\overline{(\Delta\rho)^2}$ as

$$I(Q) = C\overline{(\Delta\rho)^2}S(Q)$$

where C is a constant. Assuming that the shape of the scattering profile is invariant (as it is in this case to a good first order), then the ratio, R, of the maximum intensity, $I(Q)_t$, at a time, t, to that initially, $I(Q)_0$, yields information on the electron density difference between the phases and, therefore, provides a direct monitoring of the nanofoam formation. Then

$$R = \frac{I(Q)_t}{I(Q)_0} = \frac{\phi_{1,t}\phi_{2,t}(\rho_1 - \rho_2)_t^2}{\phi_{1,0}\phi_{2,0}(\rho_1 - \rho_2)_0^2}$$

where $\phi_{i,j}$ is the volume fraction of phase i at time j, with electron density ρ_i. The initial squared electron density difference $(\rho_1 - \rho_2)_0^2$ between the matrix polyimide and the propylene oxide is 8.32×10^{-3} mol e$^-$ cm^{-3}. The electron density of the imide matrix is 0.435 mol e$^-$ cm^{-3}. Consequently, for the ideal case where all the propylene oxide is replaced by a void, then R should be 52. From the data in *Figure 14*, an increase in the scattering by, at most, a factor of five is seen. This corresponds to a void volume fraction for the foam of only 5–6%. This is far below the initial charge of 11% and suggests that a partial collapse of the foam has occurred.

Given this partial collapse, a surprising feature in the scattering profiles is the invariance of the peak position. One would expect to see a shift in the scattering maximum to smaller Q or larger distances. It should be noted that the scattering maximum gets sharper with increasing temperature, i.e. the full width at half maximum gets smaller. This suggests that the ordering has improved somewhat. In addition, the scattering at smaller Q has increased. Taken together, these data indicate that the smaller voids have collapsed and there is a shift in the distribution of void sizes to larger sizes. However, the average separation distance between the domains has remained constant. It may also suggest either that the pores are not uniformly distributed in space according to size, or that the smaller propylene oxide microdomains are not large enough to establish effective interferences in the initial scattering profile. Nonetheless, the scattering data for these materials suggest only partial foam formation.

Some insight into the cause of partial foam formation as opposed to complete, ideal foam formation, can be gained by studying the time-resolved scattering, where the specimen is rapidly brought to a specific temperature and the evolution of the scattering is examined. Shown in *Figures 15a* and *b* are the time-resolved scattering profiles of the ODPA/FDA copolymers with propylene oxide heated to 240 and 260°C, respectively. The propylene oxide molecular weight for this sample is $\sim 2.3 \times 10^3$ g mol^{-1}. The lower molecular weight propylene oxide block was specifically chosen to investigate

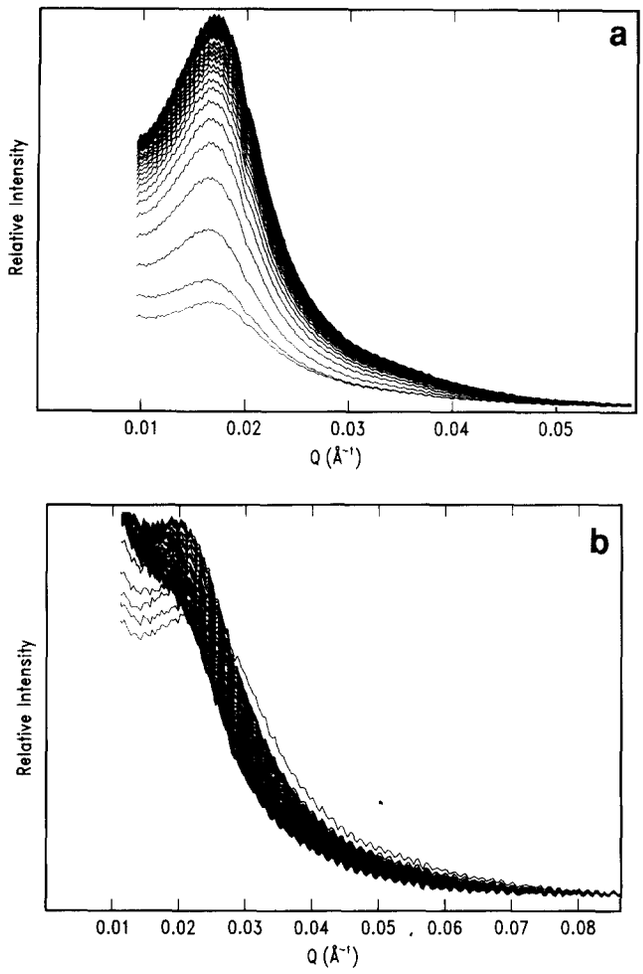

Figure 15 Time-resolved small-angle X-ray scattering profiles of copolymer **2** when the sample has been rapidly heated to (a) 240°C and (b) 260°C. Details are given in the text

the origin of the foam collapse at lower temperatures. For the 240°C data, one clearly sees the formation of the foam structure with time as evidenced by the initial rapid then more gradual increase in the scattering. For the specimen heated to 260°C, quite different behaviour is evident in the data. By the time the sample achieves thermal equilibrium (~90 s), the formation of voids is already well advanced. In fact, the initial scattering maximum is only a shoulder in the scattering profile. As time progresses, the scattering maximum is somewhat better defined, and eventually the scattering begins to decrease and a more well resolved maximum at higher Q becomes evident. The reduction in the scattered intensity is a clear indication that the foam has begun to collapse at this temperature. However, the presence of the scattering maximum shows that some of the pores are retained and they are still periodic.

From the scattering profiles, the total integrated scattering can be determined and compared to the total scattering at zero time. For the 240°C data this would show a rapid increase and then a levelling off, whereas the 260°C data would show an increase followed by a decrease in the scattering. It is most informative to compare this ratio to the weight loss data obtained as a function of time at the same temperatures. Shown in *Figure 16* is a comparison of the scattering data at 220, 240 and 260°C, to the corresponding t.g.a. data as a function of time. The t.g.a. data for these temperatures show a rapid weight loss followed by a more gradual weight loss as the propylene oxide block decomposes. The scattering data for the 220 and 240°C experiments show a rapid increase followed by an approach to a limiting value. This levelling off occurs even though more propylene oxide is being removed from the polymer. The 260°C t.g.a. data are similar to those at the lower temperatures, whereas the scattering data at 260°C show a clear decrease in the scattering. One explanation for these observations is that the decomposition products of the propylene oxide block plasticize the imide matrix. This will reduce the T_g of the imide phase to the point where, at 260°C, the experimental temperature is close to the apparent T_g of the matrix. This imparts substantial mobility to the matrix imide, and the force exerted by the surface pressure of the domains is sufficient to cause a collapse of the foam. As time progresses, the decomposition products volatilize and the remaining propylene oxide (~1%) can effectively generate a foam since the T_g of the imide phase has increased. At 220 and 240°C, the imide matrix is always below T_g and, while some of the smaller pores collapse, the larger domains are effective in sustaining the foam structure.

Consequently, the t.g.a. and scattering data together suggest that the generation of a foam is a rather subtle process. Retaining the foam structure depends upon a balance between the rate of decomposition of the propylene oxide and the rate at which the by-products can diffuse out of the matrix. If the former is greater, then the matrix is plasticized and the processing window closes by an effective reduction of the matrix T_g. If the latter is greater, then the chance of developing a nanofoam is much improved. Even in this more favourable case, however, retention of the smaller pore size does not seem possible.

Rather convincing evidence that a nanofoam can be generated via this route is shown in *Figure 17*. Here an electron micrograph of copolymer **15** with propylene oxide is shown, where the propylene oxide molecular weight is $7.9 \times 10^3\,g\,mol^{-1}$. In this figure, the porous structure of the nanofoam is clearly evident, where the white areas are voids from the degraded propylene oxide

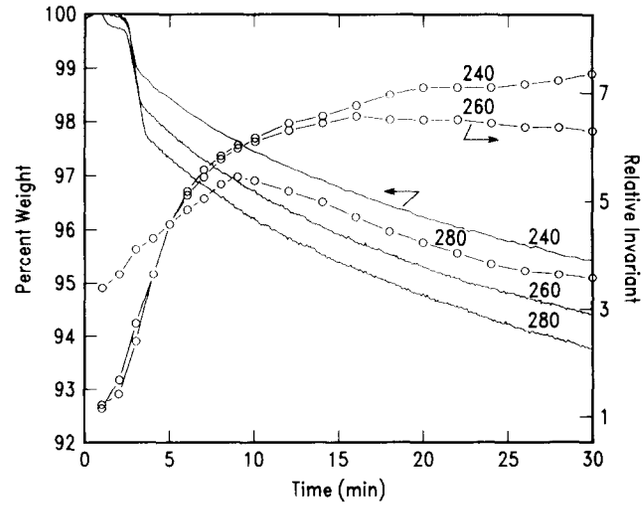

Figure 16 Comparison of the integrated small-angle scattering and the weight loss as a function of time at 220, 240 and 260°C

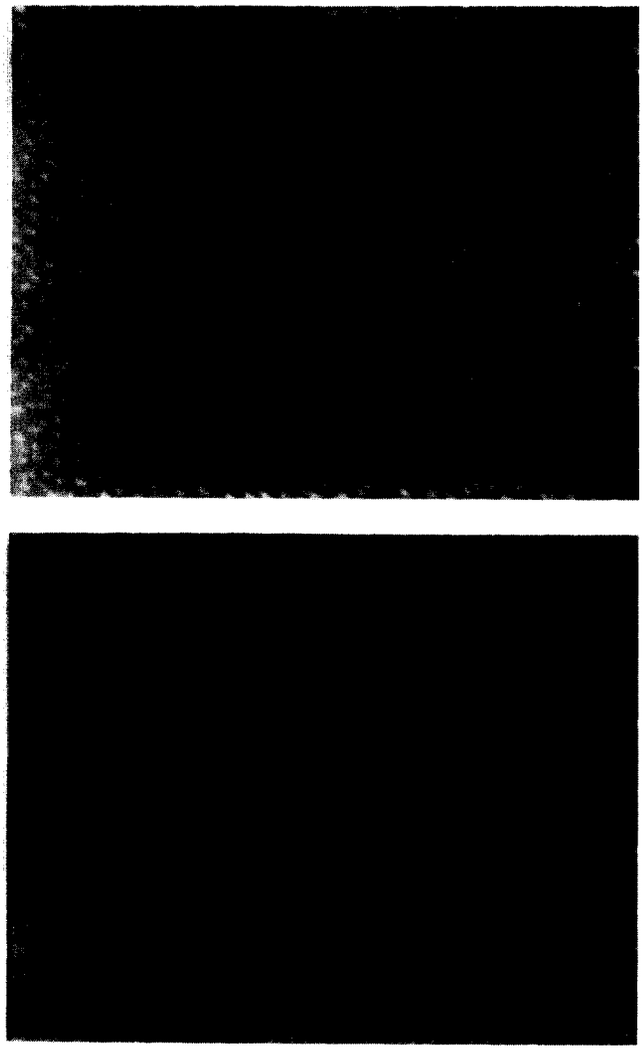

Figure 17 Electron micrographs (187 000×) of a PMDA/FDA copolymer with propylene oxide after the propylene oxide was degraded, yielding the nanofoam structure

phase. The apparent large volume fraction of the pores results from the thickness of the sample, with pores lying beneath the surface being evident as the greyish domains in the figure. The average size of the pores is ~60 Å which is slightly more than that found by small-angle X-ray scattering. However, the molecular weight of the propylene oxide is larger than that of the specimens studied by small-angle X-ray scattering. One rather important feature of these data is that the pores are not interconnected. This, as should be recalled, is critical for the end use of these materials. In addition, there is no evidence of very small pores, which is in keeping with the small-angle X-ray scattering data. Furthermore, the periodic nature of the pores is clearly evident.

In contrast to the rigid and semi-rigid polyimides, where the foam structure was observed to collapse concurrent with the decomposition of the propylene oxide coblock, foam formation was possible in the amorphous, high T_g polyimides. It should be noted, however, that the volume fraction of voids does not correspond to the volume fraction of propylene oxide in the initial copolymer. This discrepancy in the void content was also observed for the nanofoams derived from poly(phenylquinoxaline), an amorphous engineering thermoplastic, previously reported.

In both cases, a decrease in the volume fraction of voids incorporated into the matrix in comparison to the initial volume fraction of the propylene oxide in the copolymer can be understood by considering the distribution of sizes of the propylene oxide phases. Since the copolymers are not monodisperse, a distribution of propylene oxide microdomain sizes is produced. The pressure exerted on a pore will vary as γ/R, where γ is the surface tension and R is the radius. Consequently, the higher pressure on the smaller pores will tend to cause them to collapse. In addition to this, there will be a small amount of propylene oxide within the imide phase, which will be removed upon decomposition. However, this cannot account for the larger discrepancies, particularly when the initial propylene oxide content was high. In this case, the large volume fraction of the propylene oxide will necessarily give rise to smaller volumes of the imide phase between the propylene oxide phases. During the degradation of the propylene oxide, the imide can be plasticized by the decomposition products and cause a collapse of the void structure. However, the interaction of the poly(propylene oxide) degradation products with polyimide is not clear. There are approximately 11 major degradation products upon the thermolysis of poly(propylene oxide), where acetaldehyde and acetone comprise nearly 80% of these products. The calculated solubility parameters for both ODPA/FDA and PMDA/FDA polyimide, together with acetone and acetaldehyde, are shown in *Table 4*. These polyimides are polar and their solubility parameters are close to those of the major degradation products of poly(propylene oxide). In fact, ODPA/FDA and PMDA/FDA show a significant level of uptake of acetone and acetaldehyde, further suggesting a favourable interaction and the possibility of plasticization (*Table 4*). Although the duration of the plasticization may be minimal due to the elevated temperature, this transient mobility coupled with the residual thermal and solvent loss stresses are sufficient to cause a partial collapse of the foam structure. These combined observations suggest that there is an optimal void size and volume fraction that can be incorporated into the imide matrix.

SUMMARY

A new means of preparing polyimide foams with pore sizes in the nanometre regime has been demonstrated. Block copolymers comprising a thermally stable polyimide as the matrix or dominant phase with a thermally unstable material have been prepared. The copolymers were designed in such a way as to allow conventional solvent processing (e.g. spin coating and doctor blading) and, upon subsequent thermal treatment, the thermally

Table 4 Swelling of PMDA/FDA and ODPA/FDA polyimides

Sample	Calculated solubility parameter[a]	Solvent uptake (wt%)	
		Acetone	Acetaldehyde
ODPA/FDA polyimide	19.1	15.5	16.3
PMDA/FDA polyimide	19.28	33.8	–[b]

[a] Solubility parameter of acetone is 19.34 and acetaldehyde is 23.21
[b] Sample became brittle

unstable block undergoes thermolysis, leaving pores with a size and shape dictated by the initial block copolymer morphology. Triblock and graft copolymers comprising high T_g, amorphous polyimide matrices (i.e. PMDA/FDA and ODPA/FDA polyimides) with poly(propylene oxide) as the thermally decomposable coblock were synthesized. Due to the solubility of the ODPA/FDA polyimide, the ODPA/FDA imide–propylene oxide copolymers were prepared via the poly(amic acid) precursor route followed by imidization. The insolubility of the PMDA/FDA polyimide required an alternative route to well-defined block copolymers. Therefore, the poly(amic alkyl ester) route was employed as the soluble precursor to the polyimide. The triblock or graft architecture depended on the functionality of the propylene oxide oligomer used in the synthesis (i.e. mono- or difunctional, respectively). The propylene oxide compositions were deliberately maintained low so as to produce discrete domains of the thermally labile component in a high temperature polymer matrix. Microphase-separated morphologies were observed for all copolymers, irrespective of the block lengths, by dynamic mechanical analysis. The generation of the nanofoam was accomplished by subjecting the copolymer films to thermal treatment in air to decompose the propylene oxide coblock. Small-angle X-ray scattering, transmission electron microscopy and density measurements were used to assess the foam. The density values were 1–15% less than the polyimide homopolymers, consistent with the generation of a foam. Small-angle X-ray scattering and transmission electron microscopy measurements showed that the structure of the nanofoam was dictated by the morphology of the initial block copolymer. However, the volume fraction of voids was substantially less than the volume fraction of propylene oxide in the copolymer. Partial collapse of the foam was attributed to both surface effects and plasticization from the propylene oxide degradation by-products.

ACKNOWLEDGEMENT

The authors wish to acknowledge the partial support of the Advanced Technology Program of NIST under cooperative agreement 70NANB3H1365.

REFERENCES

1 Tummala, R. R. and Rymaszewski, E. J. 'Microelectronics Packaging Handbook', Van Nostrand Reinhold, New York, 1989, Ch. 1
2 Russell, T. P. *J. Polym. Sci., Polym. Edn* 1986, **22**, 1105
3 Takahashi, N., Yoon, D. Y. and Parrish, W. *Macromolecules* 1984, **17**, 2583
4 Haidar, M., Chenevey, E., Vora, R. H., Cooper, W., Glick and Jaffe, M. *Mater. Res. Soc. Symp. Proc.* 1991, **227**, 35
5 Critchlen, J. S., Gratan, P. A., White, M. A. and Pippett, J. S. *J. Polym. Sci.: Part A-1* 1972, **10**, 1789
6 Harris, F. W., Hsu, S. L. C., Lee, C. J., Lee, B. S., Arnold, F. and Cheng, S. Z. D. *Mater. Res. Soc. Symp. Proc.* 1991, **227**, 3
7 Sasaki, S., Matsuora, T., Nishi, S. and Ando, S. *Mater. Res. Soc. Symp.* 1991, **227**, 49
8 St. Clair, A. K., St. Clair, T. L. and Winfree, W. P. *Proc. Am. Chem. Soc. Div. Polym. Mater.: Sci. Eng.* 1988, **59**, 28
9 Gaghani, J. and Supkis, D. D. *Acta Astronaut.* 1980, **7**, 653
10 Smearing, R. W. and Floryan, D. C. US Patent 4,543,365 to General Electric, 1985
11 Krutchen, C. M. and Wu, P. US Patent 4,535,100 to Mobil Oil, 1985
12 Hoki, T. and Matsuki, Y. European Patent 186308 to Aashi Chem, 1986
13 Meyers, R. A. *J. Polym. Sci.: Part A-1* 1969, **7**, 2757
14 Carleton, P. S., Farrissey, W. J. and Rose, J. S. *J. Appl. Polym. Sci.* 1972, **16**, 2983
15 Alvino, W. M. and Edelman, L. E. *J. Appl. Polym. Sci.* 1975, **19**, 2961
16 Farrissey, W. J., Rose, J. S. and Carleton, P. S. *J. Appl. Polym. Sci.* 1970, **14**, 1093
17 Hammermesh, C. L., Hogenson, P. A., Tun, C. Y., Sawako, P. M. and Riccitello, R. 11th Natl SAMPE Tech. Conf. 1979, p. 574
18 Gagliai, J. US Patent 4,241,193 to International Harvester, 1980
19 Lee, R., Okey, D. W. and Ferro, G. A. US Patent 4,535,099 to IMI-Tech Corp., 1985
20 Alberino, L. M. *Cell. Plast. Conf.* 1976, **4**, 1
21 Narkis, M., Paterman, M., Boneh, H. and Kenig, S. *Polym. Eng. Sci.* 1982, **22**(7), 417
22 McWhirter, R. J. *Energy Res. Abs.* 1981, **6**, 2627
23 McIlroy, H. M. *Energy, Res. Abs.* 1977, **2**, 3469
24 Gagliani, J., Lee, R., Sorathin, U. A. K. and Wilcoxson, A. L. *Sci. Tech. Aerosp. Rep.* 1980, **18**, 37
25 Gagliani, J. and Supkis, D. E. *Adv. Astronaut. Sci.* 1979, **38**, 193
26 Hedrick, J. L., Labadie, J. W., Russell, T. and Wakharker, V. *Polymer* 1993, **34**, 22
27 Hedrick, J. L., Russell, T. P., Lucas, M., Labadie, J. and Swanson, S. *Polymer* in press
28 Volksen, W., Yoon, D. Y., Hedrick, J. L. and Hofer, D. *Mater. Res. Soc. Symp. Proc.* 1991, **227**, 23
29 Russell, T. P. in 'Handbook of Synchrotron Radiation' (Eds G. S. Brown and D. E. Monctar), North Holland, Amsterdam, 1991, Vol. 3
30 Rogers, M. E., Moy, T. M., Kim, Y. J. and McGrath, J. E. *Mater. Res. Soc. Symp. Proc.* 1992, **264**, 13